Nanotechnology Perceptions
ISSN 1660-6795
www.nano-ntp.com

Analytical And Bioanalytical Approaches For Evaluation Of Nanoparticulate Formulation

Bhavana Wani[1], Sonali Mahaparale[2]

[1-] Research Scholar, Dr. D. Y. Patil College of Pharmacy, Akurdi, Pune-411044
[2-] Associate professor, Dr. D. Y. Patil College of Pharmacy, Akurdi, Pune-411044

The aim of this effort is to increase extended pharmaceutical release by systematizing PN elaboration for Memantine, a novel treatment for Alzheimer's disease. The original QTTPs and CQAs were recognized and their existence was justified by the QbD method. The data was methodically adjusted using the BBD once the initial screening process utilizing Taguchi screening was completed. The regression equation and response surface were examined. An ANOVA model was used to pinpoint a particular crucial model term. The high and low value ranges for various CQAs were coded in order to maximize the freeze-dried PNs of Memantine. An overlay plot was used to confirm the identity of the design space. BBD was used to create the ideal single dosage of freeze-dried powdered nails (PNs), which included 30 mg of Memantine, 30 mg of PLGA, and 1.5% w/v of poloxamer-188. The optimized freeze-dried PN formulation was assessed and found to have an ideal particle size of 148.90 nm, a ZP of 23.8 mV, an EE of 70.57%, and a 24-hour in vitro drug release of more than 75%. The findings pertaining to drug levels in the brain, both in vitro and in vivo, unambiguously demonstrated that the proposed methods allow for a sustained delivery of the treatment into the target region. The bio adhesive polymer properties of the identified colloidal systems demonstrate that the NPs are appropriate for oral administration and enhance the quantity of medication that reaches the target organ. Furthermore, it was demonstrated that a different distribution schedule (on different days) could be able to achieve therapeutic drug concentrations in the brain. Studies on the behavior and histology of WT and NP-treated APP/PS1 mice on various days revealed that NPs groups performed better in improving the APP/PS1 animals' learning capacities and -amyloid brain plaques than free MEM therapy. This is the result of the targeted organ receiving a consistent dosage of medication from MEM-PLGA NPs through their extended release.

Keywords: Alzheimer's disease, Memantine, PLGA, Nanoparticles, Analytical, QbD, Bioanalytical, etc.

Introduction

The most prevalent kind of dementia is Alzheimer's disease. This neurological disorder results in memory loss and cognitive deterioration due to neuronal atrophy. Those over 65 are typically affected by the illness. Medication solely addresses the symptoms of Alzheimer's disease, lessening discomfort and enhancing life expectancy. Cholinesterase inhibitors are a class of medications used to treat a number of ailments, such as memory loss, confusion, altered brain chemistry, and impaired judgment. They enhance neuronal connections throughout the brain and reduce the duration of some symptoms [1, 2].

Apart from the aforementioned causes, the development and course of AD can also be influenced by genetic susceptibility, hormone issues, mitochondrial dysfunction, and calcium toxicity. In order to address the symptoms of Alzheimer's disease, a variety of active pharmaceutical ingredients (API) have been suggested recently. These include phosphodiesterase and cholinesterase inhibitors, antioxidants, non-steroidal anti-inflammatory drugs (NSAIDs), tau hyperphosphorylation inhibitors (e.g., methylene blue, methylene blue-like GSK3 serine-threonine kinase inhibitors), intracellular NFTs inhibitors, estrogenic hormones, insulin-opposing medications, metallic chelators, vitamins, stem cells, and neurotrophies (e.g., BDNF, brain-derived neurotropic issue) [3–8].
The selective nature of the blood-brain barrier (BBB), which keeps many central nervous system (CNS) medications from penetrating the brain, is one of the primary barriers to the development of effective drugs for the prevention and treatment of AD. An essential step in the research, development, and production of pharmaceuticals is the establishment and validation of analytical methods. The approved test methods that come from these processes are used by quality control laboratories to make sure that pharmaceutical products are recognized, pure, powerful, and efficient. They include all the steps required to prove that a specific method for the precise and reliable measurement of analytes in any biological matrix—blood, plasma, serum, or urine, for example—is appropriate for the intended use. Numerous papers [9–12] have demonstrated the importance of sample throughput in the development of bioanalytical procedures incorporating effective preparation.

Memantine (MEM) has potential as a medication loader. MEM is an NMDA receptor antagonist with low to moderate affinity that binds preferentially to cation channels that are regulated by NMDA receptors and that cross over into the magnesium site. It is an uncompetitive (open-channel) NMDA receptor antagonist. Consequently, MEM lowers the elevated glutamate that causes neuronal death in AD patients [13]. However, the results of a meta-analysis of AD monotherapy show that this medication has limited clinical benefits (i.e., there was no statistically significant difference in assessment scores between the treated and non-treated groups) [14]. This medication was found to improve patients' cognition, behavior, and stage of dementia in contrast to placebo groups. Drug delivery tools would increase the drug's concentration at the desired location in this manner, potentially enhancing its anti-AD benefits. Additionally, although though MEM is well-tolerated, it requires daily patient administration, which can further reduce treatment success rates when combined with insufficient drug adherence.

In addition to helping to give a time-stable dosage on the brain, it is hoped that PLGA NPs will extend pharmaceutical release, reduce the frequency of administration, and diminish unfavorable side effects. Oral administration improves patient compliance and is more comfortable for patients when it comes to long-term treatment programs. Recent studies have demonstrated the advantages of loading drugs into PLGA NPs to boost their oral bioavailability [15, 16]. When administered orally, PLGA NPs help increase the drug's bioavailability due to their enhanced ability to permeate mucus [17].
We report here the development of a physicochemically stable, sustained-release formulation of MEM–PLGA NPs for the treatment of AD. Targeting MEM in the brain with developed

MEM-PLGA NPs is said to provide a non-invasive, minimally invasive approach. The physicochemical stability of MEM after loading in PLGA NPs has been ascertained using both in vitro release profiles and drug-polymer interaction tests. Cell survival was investigated and the blood-brain barrier's in vitro transit was mapped. Both transgenic and non-transgenic mice were given MEM-PLGA NPs orally, and the results were compared to those of treatment with a free drug solution. The therapeutic efficacy of MEM–PLGA NPs for brain delivery was evaluated by tracking medication concentrations in the brain and plasma, as well as by performing behavioral tests and histological analyses in comparison to free medicine.

Material and Method

Materials

We bought Memantine from A. S. Joshi and Company in Mumbai. PLGA was given as a gift sample by Dr. Reddy's lab in Hyderabad, India. Poloxamer-188 was supplied by Mumbai, India-based Himedia. Mannitol was supplied by Mumbai, India-based Himedia Chemicals Pvt. Ltd. Furthermore, the highest caliber and analytical grade reagents, solvents, and necessary compounds were used in this inquiry.

Methods

Preliminary screening of influential factors using Taguchi design

The basic screening was conducted utilizing a combination of the 7-factor, 2-level Taguchi design in an attempt to determine the significant vital factor(s) affecting the CQAs. For the Taguchi design, an eight-formulation combination was developed and suggested.

Preparation of Polymeric nanoparticles (PN) formulation

The creation of PNs was attempted utilizing the ultra-sonication method after nano precipitation. The required quantity of PLGA was dissolved in the organic phase (acetone) at 50°C and then added to the Memantine acetone solution. The organic phase was added drop wise, at a rate of 3 mL per minute, to the poloxamer-188 (aqueous phase) additive solution using a glass syringe fitted with a gauge size 26 needle. The mixture was stirred at a rate of 5000–15,000 rpm at 25°C. The ultrasonic state parameter was set at 3 s at a 2 s interval at 40 W for five minutes. A Rotary evaporator was used to evaporate the remaining acetone for two minutes at 40°C at condensed pressure. The resultant nanosuspensions were centrifuged at 9000 rpm for 10 minutes.

Systematic formulation optimization studies

The BBD response surface design with three variables and three levels of mixture components was taken into consideration for optimizing the PN formulations. Design Expert ver. 12.1.1 software (Stat Ease, Minneapolis, MN, USA) was utilized to create the experimental trials. The independent variables or parameters that were employed were the ratio of Drug: PLGA (mg) (X1), poloxamer-188 concentration% w/v (X2), and stirring speed (X3). To calculate the substantial impact of these several variables or responses, such as cumulative% drug release QT24%, three levels (-1, 0 and 1) were constructed. Additional CQAs were created for

examination in addition to five consecutive cumulative replicates of the centre point trial and a total of 17 trial formulations.

Lyophilisation of optimized PNs

A large body of research indicates that the lyophilized materials have a porous structure with enhanced redispersibility and long-term stability [81]. For run no. 16, a lyophilizer using ALPHA 1- 2 LO Plus CHRIST was used to create the powdery freeze-dried state at a pressurized vacuum of 0.01 KPa for roughly 48 hours at -50°C to achieve a drug-loaded lyophilized PNs. Once the optimized formulation was freeze-dried to a powder using the suitable cryoprotection—in this example, 2% Mannitol—it was subjected to micrometric characterization.

Characterization of freeze-dried PNs

Fourier-transform infrared spectroscopy (FT-IR)

Using FT-IR spectroscopy, it was possible to assess the possible physical interactions of the medicine Memantine. The FT-IR spectra of selected Memantine and physical mixes (PM) including PLGA and poloxamer-188 were recorded using KBr at a resolution of 4 cm-1. To investigate the drug-excipient compatibility, the transmittance range between 4000 and 400 cm-1 was calculated. To identify and assess any noteworthy interactions between Memantine and the other additives, peak matching was employed [23].

Differential scanning calorimetry (DSC)

DSC tests were performed to assess the interaction between the drug and the polymer. All of the required samples (10 mg) were heated in aluminium pans using effluent gas that contained dry nitrogen. Calculations were made about the excipients' DSC thermogram, matching PMs, and the pure Memantine medicine [24].

Entrapment efficiency (EE)

It was feasible to forecast the percentage EE of Memantine in the formulated or manufactured PNs by measuring the Memantine content in the PNs. Samples of 10 mL of Memantine PNs were centrifuged for 30 minutes at -4°C at 9000 rpm using a cooling centrifuge. The free, encapsulated medicine can be extracted by centrifugation dialysis [84]. The supernatant free drug was calculated and verified at 222 nm using the UV-spectrophotometric method. To ascertain and compute the drug EE (DEE) or (DEE %) of nanoparticles, utilize equation (1).

% Entrapment Efficiency = (Total amount of drug-Free Drug)/ (Amount of total drug content) × 100……. (Eq.1)

Particle size and ZP measurement

Particle size, polydispersity index, and ZP were effectively assessed by Photon Correlation Spectroscopy using the Zetasizer Nano-ZS Make-Malvern apparatus. ZP implies that there may be a relationship between the system value and the stability of colloidal dispersions. The

stability or immobility suggested for molecules and sufficiently small particles will be demonstrated by a high ZP [25].

In-vitro diffusion studies

This in-vitro drug release study employed the dialysis bag diffusion method for the pure medicine Memantine. After being hermetically packed in a dialysis bag, formulas (5 mL) were poured into 150 mL of 0.1 N HCl under sink conditions for the first two hours. After that, it was immersed in a 6.8 pH phosphate buffer solution for a whole day. The system was continuously magnetically agitated at 200 rpm and maintained at 37°C. A sample (2 mL) was pipetted out of the receptor's compartment at predefined intervals and replaced with an exact volume of brand-new pH 6.8 phosphate buffer and 0.1 N HCl. This 1 mL sample was then mixed with 1 mL of ethyl acetate. After the material was vortexed in a cyclomixer, 0.5 mL of the solution's supernatant layer was generated in a test tube. After being allowed to dry for a while, the mobile phase was added, and the test tube was examined using RP-UFLC. A non-Fickian diffusion mechanism, along with a concentration gradient, diffusion mechanics, and swelling degree, were used to analyse kinetic investigations [26, 27].

Solid-state characterization

Powder X-ray diffraction (P-XRD)

The P-XRD (Rigaku, Japan, Smart Lab 9 kW) was utilized for the diffraction studies. The P-XRD tests were performed on the materials by subjecting them to nickel-filtered CuKa radiation (40 kV, 30 mA), which made the scan possible. For the P-XRD-related investigation, the pure medication and optimized lyophilized powdered minerals (PNs) of Memantine were required. The results were then plotted as peak height (intensity) against time (h).

Scanning electron microscopy (SEM)

SEM examines a nanoparticle's exact appearance or surface polish. A high-resolution SEM was used at 30 kV. The formulation bearing that has to be tested is attached to the carbon-coated metallic stub. SEM is useful for a detailed examination of surface morphology. A high-energy electron is used to scan the surface of an Au and Pt-coated specimen in order to improve contrast and signal-to-noise ratio. To determine surface morphology, pure medicine and optimized lyophilized PNs were thoroughly examined in the interim [28].

Transmission electron microscopy (TEM)

The outer appearance or shape of the PNs of Memantine could be ascertained by TEM after they were lyophilized, diluted with 2 mL of distilled water, and completely mixed by ultra-sonication for 3 minutes. A drop of Memantine PNs was placed onto a coated copper grid to set up the samples, and they were then let to air dry [29].

Thermogravimetric analysis (TGA)

TGA tests were utilized to support the moisture content associated with weight loss in isothermal or non-isothermal stability investigations. TGA suggests that it's critical to ascertain and measure the amount of moisture content in pharmaceutical formulations. In the early

phases of Preformulation research, it is thought to be a reliable technique for differentiating polymorphs from hydrates or identifying monohydrates among other hydrates, tasks that DSC alone might not be able to accomplish [30].

Differential thermal analysis (DTA)

It is imperative that polymorphisms be examined and drug stability, solvation, degradation, compatibility with excipients, and impurity investigations be forecasted utilizing thermal analytical techniques. Additionally, melting point determination is said to be improved by DTA, a thermal approach that has been around for a while [31].

Cell culture

Under a microscope, cells had to be continuously defrosted, developed, maintained, and observed. The two cell lines used were astrocytes from the rat cortical brain and mouse microvascular endothelial cells (bEnd.3). Primary astrocyte cultures were obtained using a bank GAIKER-IK4 culture. The growth media used to maintain the viability of the bEnd.3 cells was DMEM+10% FBS [32]. After heating the cells and related culture media to 37 ℃, a centrifuge was used to separate the cell suspension at 4 ℃ for 5 minutes at a speed of 130g. The supernatant was discarded and the cells were once again suspended in culture media. After being seeded, 75 cm2 flasks containing cells were kept in an incubator at 37 °C, 5% CO2, and a relative humidity of 80 %.

Cytotoxicity studies

Alamar blue reduction was used to test the vitality of the cells. The premise of this test is that metabolically active, living cells transform resazurin into resorufin, which is subsequently released into the culture medium. The oxidoreductases found in the cytoplasm, microsomes, and mitochondria enable this intracellular conversion. In a dangerous occurrence where there is a loss of cell viability and proliferation, the epithelial tissue's constituent cells are unable to lower resazurin. Consequently, there is a direct inverse relationship between the number of viable cells and the resazurin reduction ratio. The absorbance was measured in reduced and oxidized forms at 570 and 620 nm, respectively [32]. Data were analysed by computing the percentage of Alamar blue decline and expressing the results, as previously described [33].

In vitro transport across the BBB

In vitro BBB models are a popular method for assessing a drug's ability to cross the BBB early in the drug development process. The current study improved endothelial cell-based models by co-culturing astrocytes and endothelial cells in Tran's well systems. Using polycarbonate Trans well inserts, a semipermeable membrane with a 0.4 m pore size was used. For the co-culture tests, endothelial cells were seeded in the apical region of the inserts. Rat astrocyte primary culture cells were added to a semipermeable filter's basolateral compartment.

Trans-epithelial electrical resistance study

The brain vasculature is composed of endothelial cells with strong, tight connections that selectively limit the paracellular diffusion of hydrophilic molecules according to their size and charge. When the barrier operates correctly and restricts the ion flow, an electric potential

gradient is generated on both sides of the monolayer. A measure of cell confluence, monolayer integrity, and the formation of tight connections is Transepithelial electrical resistance, or TIER. Thus, using a pair of STX2 electrodes, epithelial EVOM2 voltmeter measurements were manually taken each day until a steady state was reached. The gadget is operated by two electrodes that are immediately inserted into the inserts. The TEER of every insert was calculated using Equation, and the results are shown in Ω cm2.

$$TEER = \left[\Omega_{cell\ monolayer} - \Omega_{Filter\ (without\ cells)}\right] \times [Filter\ Surface]$$

Co-culture experiments were conducted using 24-well plates. Fresh media plates containing Hanks and 0.5% bovine serum albumin (BSA) were used to hold the removed inserts. After removing the top media from the inserts and rinsing them with Hanks, MEM-PLGA NPs (dissolved in 0.5% BSA Hanks) were added and the inserts were allowed to sit for an hour. At the end of the study, Lucifer yellow (LY), a material with limited paracellular permeability, was added to ensure that MEM-PLGA NPs did not compromise membrane integrity. The permeability coefficient was determined using the clearance principle, which allows a permeability value to be independent of concentration and is used to assess membrane integrity (with LY).

In-vivo studies

C57BL/6 and male APPswe/PS1dE9 (APP/PS1) mice were used in the in vivo study. Mice that coexpress the Swedish (K594M/N595L) mutation of a chimeric mouse/human APP (Mo/HuAPP695swe) and the human exon-9-deleted version of PS1 (PS1-dE9) are able to produce higher amounts of human A peptide. The animals had unrestricted access to food and water and were housed in conditions with regulated lighting, humidity, and temperature. The regulations of Ramaderia, Pesca, the Department of Agriculture of the Generalitat de Catalunya, and European Community Council Directive 86/609/EEC were followed for handling mice. Every effort was undertaken to reduce the quantity of animals used and their suffering. Six sets of six-month-old mice were employed in this study, each consisting of at least ten WT and ten APP/PS1 transgenic mice. Treatments for the mice in each genotype group included untreated water, free MEM, or MEM NPs. Mice received MEM daily at the prescribed dose of 30 mg/kg for two months. On different days, MEM-PLGA NPs were given orally, and each rat received a regimen of untreated water after their weight was determined. After the in vivo tests, the animals were euthanized. Before being slaughtered, mice were permitted to starve for a minimum of eight hours, or longer if they were given medication. At least six mice from each group were used for the histopathological analyses [34].

Nanoparticles brain distribution

To prevent NP uptake and visualize MEM NPs in the target region in vivo, PLGA was conjugated to Rhodamine to designate the NPs fluorescently. After receiving NPs orally for a week on alternate days, mice were put to sleep with sodium pentobarbital and then infused with 4% paraformaldehyde. Overnight at 4 °C, brains were kept dehydrated in a 30%

phosphate-buffer sucrose solution. Samples were maintained at 80 °C until coronal slices of 20 m were cut using a cryostat (Leica Microsystems, Wetzlar, Germany). The samples were viewed using a fluorescent microscope equipped with a Rhodamine filter (BX41 Laboratory Microscope, Melville, NY-Olympus America Inc). Prior to the examination of the therapeutic effects, drug levels at steady state were determined. After drawing blood from a facial vein, samples were spun for 20 minutes at 2000 rpm with EDTA added to stop the blood from clotting. Mice were killed by dislocating the cervical disc. Amantadine served as an internal reference during the MEM extraction process, which was conducted using organic solvents (t-butyl methyl ether and diethyl ether-chloroform for the brain and blood samples, respectively). Solvents were evaporated under nitrogen flow, and samples were then reconstituted with methanol [35, 36]. As previously mentioned (in section NPs production), the samples were analyzed. The investigation was conducted using parent to daughter pairings of m/z 180>163 (MEM) and m/z 152>135 (amantadine).

Morris water maze

A circular tank that had been partitioned into four equal quadrants and filled with water at 21 °C was used to conduct the Morris water maze (MWM) test. A white platform lay beneath the surface of the water in the northeastern quadrant's centre. Utilizing an automated video monitoring system, behavioural data was gathered and analyzed. The behaviour evaluation technique consisted of a probing trail and a six-day navigation testing session. The mice were kept on the same drug regimen and underwent five trials per day for six days in a row. Animals were placed inside the maze at water level, their backs facing the tank wall. After swimming freely for 60 seconds to find the concealed platform, they were allowed to stay there for ten seconds. If the mouse did not discover the platform on its own, it was led to it and held there for 30 seconds. The probe trial was held on the day after the final training exam. When the hidden platform was removed for the probing test, the mice were released from the southwest quadrant and given 60 seconds to swim. The outcomes for each animal were computed independently [37].

Immunohistochemistry studies

Mice were rendered unconscious with sodium pentobarbital after the probing procedure, and then they were given 4% paraformaldehyde in 0.1 M phosphate buffer (PBS). Brains were stored in 4% paraformaldehyde at 4 °C for the whole night before being dehydrated in a 30% phosphate-buffered sucrose solution for cryoprotection. Samples were maintained at 80 °C until coronal slices of 20 m were cut using a cryostat (Leica Microsystems, Wetzlar, Germany). Prior to being incubated with the Alexa Fluor 594 goat anti-rabbit antibody (1:500; Invitrogen, Eugene, OR, USA) for two hours at room temperature, sections were first incubated with the primary rabbit anti-GFAP antibody (1:2000; Dako, Glostrup, Denmark) for an entire night at 4 °C. In order to compare the density of amyloid plaques in different treatment groups, amyloid plaques were stained with tiofavin S (TS 0.002%, Sigma-Aldrich). After counterstaining with 0.1 g/ml Hoechst 33,258 (Sigma Aldrich, St. Louis, MO, USA), sections were cleaned with PBS 0.1 M [38]. TS-stained amyloid plaques were viewed using a fluorescent microscope equipped with a fluorescence filter (BX41 Laboratory Microscope, Melville, NY-Olympus America Inc.). For every image, the proportion of the entire image that was filled

with fluorescently dyed amyloid plaques was calculated. Each mouse had four representative fields per slice, and the average plaque concentrations of those fields were computed [39].

Accelerated stability study

According to ICH guidelines, the optimized nanoparticle dosage form was put through accelerated stability studies utilizing a stability chamber (TH200G, Thermolab, Thane, India) for six months at 40°C and 75% relative humidity. The samples were carefully removed from the stable at 0, 1, 2, 3, and 6-month intervals and assessed for drug release, ZP, and particle analysis.

Analytical and Bioanalytical Study

Instrumentation

An LC-MS system with the Shimadzu® UFLC series trademark was linked to a PC running Lab Solutions LCMS® Software (version 5.42 SP4 for LCMS-2020) (Shimadzu Corporation, Kyoto, Japan). A control unit (CBM-20A), two pumps (LC-20AD), a degasser (DGU-20A), a UV detector (SPP-20A), a column oven (CTO-20AC), a thermally controlled auto sampler (SIL-20AC), and an MS detector (LCMS-2020) were among the parts of the system. ACE Excel2 C18 (100 ×3.0 mm) (ACE®), a column with a particle size of 2 µm, was used.

Chromatographic conditions

Utilizing a C18 column (100 ×3.0 mm) with a particle size of 2 µm and an isocratic flow rate of 0.4 mL min-1, a mobile phase system comprising 20% ammonium formate buffer pH 9.5 (0.1% formic acid in water adjusted to pH 9.5 with ammonium hydroxide) and 80% methanol was employed. The chromatograms were retrieved using an ESI (electrospray ionization) interface with an MS detector in SIM (single ion monitoring) mode and positive polarity at m/z 289 (for Memantine) and 359 (for NLB). All computations are done at 40 °C. Memantine and NLB had elution times of 1.8 and 2.9 minutes, respectively.

Statistical analysis

To make group comparisons easier, a two-way ANOVA was followed by a Tukey post hoc test. To compare the two groups was the aim of the Student's t test. GraphPad Prism version 5.00 for Windows was given by GraphPad Software, San Diego, California, USA, and the statistical significance threshold was set at $p < 0.05$.

Result and Discussion

Drug and excipient interaction study

Fourier Transformation Infrared Spectroscopy (FTIR)

FTIR spectrum of Memantine was shown in following Fig. revealed that the characteristic peaks representing the presence of functional groups claim by its chemical structure. From this we can consider that the Memantine was of pure quality.

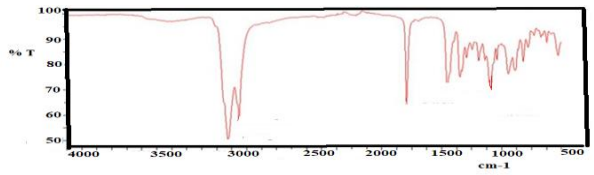

Fig. FTIR spectra of Memantine

After interpretation of FT-IR Spectrum of Memantine it was concluded that all the characteristic peaks corresponding to the functional group present in the molecular structure of Memantine were found within the reference range and confirming its identity.

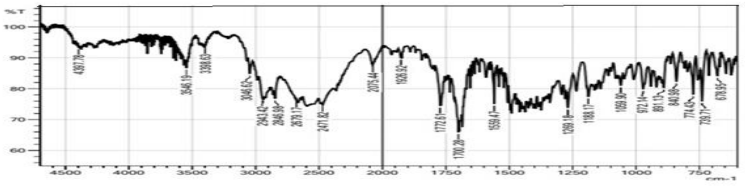

Fig. FTIR spectra of physical mixture (Memantine + PLGA)

After interpretation of FT-IR Spectrum of PLGA and its physical mixture with drug, it was concluded that all the characteristic peaks corresponding to the functional group present in molecular structure of Memantine were not found intact within the reference range, confirming its reactivity with PLGA. This interaction further supports the selection of polymer.

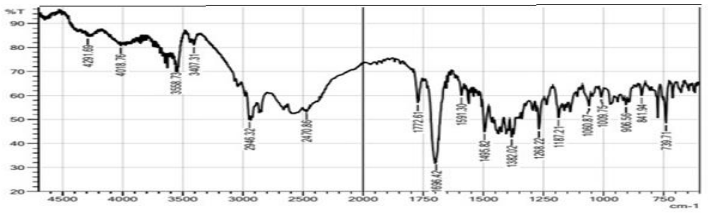

Fig. FTIR spectra of physical mixture (Memantine + Poloxamer 188)

After interpretation of FT-IR Spectrum of Poloxamer 188 and its physical mixture with drug, it was concluded that all the characteristic peaks corresponding to the functional group present in molecular structure of Memantine were not found intact within the reference range, confirming its reactivity with Poloxamer 188. This interaction further supports the selection of polymer.

Differential Scanning Calorimetry (DSC)

The thermal analysis of Memantine was studied by using DSC as shown in following figure. Respectively. The Memantine shows an endothermic peak at approximately 282℃ and it corresponds to its melting point.

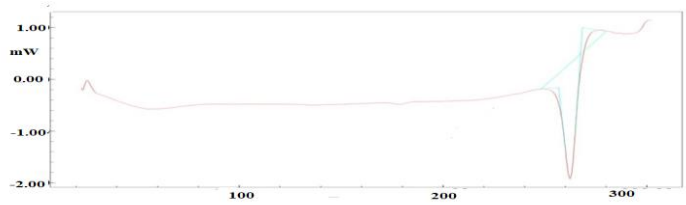

Fig. DSC thermogram of Memantine

Taguchi screening design for identifying critical factors

In the initial screening (Taguchi OA design), two levels were selected for low and high (1 and 2) in order to eliminate the most crucial characteristics. Table 1 shows the corresponding coded and real values for the formulations based on the CQAs. The impacts of a number of variables were examined, including A-PLGA concentration, B-poloxamer-188 concentration, C-speed of stirring, D-time of stirring, E-time of Ultrasonication, F-temperature, and G-type of stirring. The p values of the regression coefficients (R2) were determined in order to evaluate the significance of each component for each answer. For the model factors A, B, and C, the model terms are significant since the p value is less than the standard value (0.05), but not for other factors with p values greater than 0.1000. Thus, from the factor screening analysis, the parameters A-Drug: PLGA concentration, B-Poloxamer-188 concentration, and C-Stirring speed were ultimately selected as important factors for further optimization.

Table 1: Design matrix for factor screening as per Taguchi design along with the experimental results of various CQAs and factors with their respective low and high levels

Runs	**A**	**B**	**C**	**D**	**E**	**F**	**G**	**QT24 %**	**Particle size (nm)**	**ZP (mV)**	**PDI**
1	2	1	2	1	2	1	2	48.984	253.5	-28.9	0.300
2	2	2	1	1	2	2	1	68.343	182.1	23.33	0.176
3	1	2	2	2	2	1	1	33.342	277.4	-23.4	0.357
4	2	2	1	2	1	1	2	73.904	192.6	19.232	0.128
5	1	1	1	2	2	2	2	48.786	267.8	-23.4	0.369
6	2	1	2	2	1	2	1	71.235	225.2	-18.313	0.222
7	1	1	1	1	1	1	1	60.235	267.8	-24.7	0.369

8	1	2	2	1	1	2	2	64.457	287.8	-30.2	0.654

Factors	**Codes**	**Low level (-1)**	**High level (+1)**
PLGA concentration (mg)	A	20	60
Poloxamer-188 concentration (gm %)	B	0.5%	1.5%
Stirring speed (rpm)	C	5000	10000
Stirring time (h)	D	1	2
Ultrasonication time (min)	E	5	10
Temperature °C	F	25	40
Stirring type	G	Magnetic	Mechanical

CQAs: Critical quality attributes, PLGA: Poly-lactic-co-glycolic acid, PDI: Polydispersity index, ZP: Zeta potential

Experimental design, optimization, and analysis

While keeping the other variables at a low level, the PLGA, poloxamer-188, and stirring rate concentrations were changed. Based on early results from the Pareto chart analysis, three levels (-1, 0 and 1) were selected for each of the components. Table 2 presents a 33 BBD three-level three-factor application with a total of 17 runs. Characterization studies of each formulation were performed to ascertain the effect of several factors on specific CQAs, such as A-Drug: PLGA concentration, B-Poloxamer-188 concentration, and C-Stirring speed.

Table 2: Composition of various Polymeric nanoparticles of Memantine as per BBD along with the obtained CQAs responses and their coded levels QT24 % cumulative % drug release at 24 hr.

Runs	**Factor 1**	**Factor 2**	**Factor 3**	**Response Y1**	**Response Y2**	**Response Y3**	**Response Y4**
	A:X1 PLGA: Drug ratio (mg)	**B:X2 poloxamer -188 concentration (%w/v)**	**C:X3 stirring speed (rpm)**	**QT24 %**	**Particle size (nm)**	**Zeta potential (mV)**	**PDI**
1	-1	0	-1	61.346	391.312	14.24	0.454
2	1	0	-1	36.693	349.782	-22.22	0.433
3	0	0	0	49.825	346.454	-19.29	0.429

4	1	1	0	39.568	169.313	-22.7	0.390
5	-1	-1	0	63.543	433.368	-11.325	0.643
6	0	1	1	61.322	233.346	-19.675	0.300
7	0	1	-1	46.433	237.545	-20.422	0.350
8	0	-1	-1	43.872	451.212	-12.985	0.654
9	0	0	0	54.568	335.022	-16.28	0.258
10	0	0	0	55.988	324.238	-16.312	0.235
11	0	0	0	56.343	294.246	-17.323	0.232
12	-1	0	1	68.312	291.313	-7.322	0.172
13	1	-1	0	38.986	433.212	-21.4	0.635
14	1	0	1	30.412	287.769	-22.25	0.128
15	0	0	0	60.094	291.579	-19.432	0.232
16	-1	1	0	77.946	148.900	23.8	0.399
17	0	-1	1	45.253	404.232	-13.235	0.544

Independent variables	**Levels**		
	Low level (-1)	**Middle level (0)**	**High level (+1)**
X1: Drug: PLGA ratio (mg)	1:1(30 mg)	1: 1.5 (45 mg)	1:2 (60 mg)
X2: Poloxamer-188 concentration (%)	0.5 %	1 %	1.5 %
X3: Stirring speed (rpm)	5000	10000	15000

PNs: Polymeric nanoparticles, MEM- Memantine, BBD: Box-Behnken Design, CQAs: Critical quality attributes, PDI: Polydispersity index, PLGA: Poly-lactic-co-glycolic acid

Response surface analysis of 2D and 3D plot

Effect of the factor on CQA QT 24 %

Figure a displays the 2D (contour) and 3D graphs for the CQA QT24%. After extensive analysis, it has been determined that the red zone will predominate at low drug concentrations (-1) of PLGA and high drug concentrations (1) of poloxamer-188, with over 75% of the drug being released in a 24-hour period. For run number 16, the maximum medicine release percentage is 77.946%. Owing to the elevated content of Drug: PLGA at level (1), Run No. 14 exhibits a minimum QT24% value of 30.412%. Particle aggregation and size distribution increase with increased polymer concentration, slowing the release behaviour. The results indicate the ideal drug concentration: For the best drug solubility, a higher polymer ratio is required. Furthermore, it can be concluded that the concentration of the stabilizer (poloxamer-188) has a major impact on the improved drug solubility.

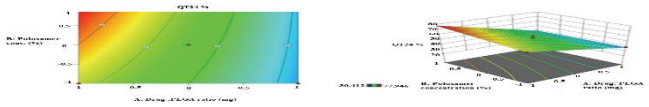

Fig. a

Effect of the factor on CQA PS

Figure b displays the 2D (contour) and 3D plot of the CQA. PS: For runs 16 and 8, the particle sizes are 148.900 nm and 451.212 nm, respectively. The blue zone illustrates that the lower range of particle size is reached at high level (1) of B-poloxamer-188 concentration and low level (-1) of factor A-Drug: PLGA concentration. As the dark yellowish zone indicates, it is reasonable to assume that at lower concentrations of A-Drug: PLGA, a reduction in particle size is effectively achieved, and that this characteristic becomes considerably more pronounced at higher concentrations. An increase in the stirring rate has an impact on the particle size, or size decrease.

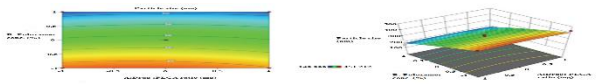

Fig. b

Effect of the factor on CQA ZP

Figure c displays the CQA polydispersity index (PDI) as 2D (contour) and 3D plots. The CQA ZP appears to be impacted by both the concentration of B-poloxamer-188 and the concentration of A-drug: PLGA. At a low level of 0.5 of A-Drug, it ranges between -7.322 mV for run 13 and 33.8 mV for run 16. The concentrations of PLGA and B-poloxamer-188 at more than level 1 show greater values, which are predicted to have a substantial effect on the CQA.

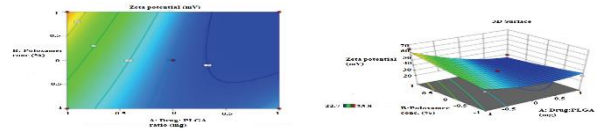

Fig. c

Effect of the factor on CQA PDI

Figure D displays the contour plot and 3D plot of the CQA PDI. A-DRUG: PLGA and B-poloxamer-188 concentrations seem to affect the PDI similarly. Values for runs 14 and 8 range from 0.13 to 0.66. The results showed that the PDI value only remains below 0.2 when the B-poloxamer-188 and the A-drug, PLGA, concentrations are both greater than 0.5. Uniform size distribution is essential for a medication to be absorbed at the GI membrane. It is the stabiliser system's job to keep the size distribution regular.

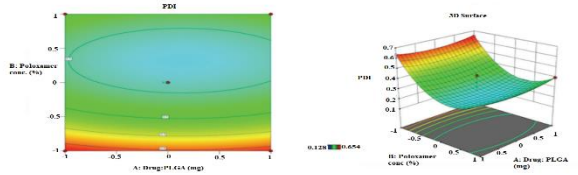

Fig. d

Fig. Contour plots (2D) and response surface plots (3D) of selected independent factors on selected dependant factors: QT24 % (a); particle size (b); zeta potential (c), and polydispersibility index (d)

Analysis of variance (ANOVA) of BBD design

The ANOVA findings for each component were compiled, and their importance with respect to the quadratic model was determined. After the design matrix is finished, the final model F values for QT24%, PS, ZP, and PDI are calculated to be 22, 77, 12,81, 6,07, and 6,73, respectively. The fact that P values for the model for various CQAs were less than or equal to 0.05 (=0.05) shows the importance of the quadratic model. The lack-of-fit p values for ZP, PDI, PS, QT24%, and 0.002 were computed to be 0.456, 0.002, 0.566, and 0.158, respectively. It is not significant in terms of pure error (i.e., p value >), which is better for a fitting model. For the CQA QT24%, model terms like A, B, and C2 are crucial. For the CQA PS, model term B is crucial. Three important ZP model terms are A, AB, and A2. In PDI, model terms like B, AB, and B2 are just as significant as CQA. If the P value for the model terms is less than 0.05, they are deemed significant.

Summary of BBD quadratic model

During the optimization process, the BBD quadratic model summary is used to optimize the Memantine PNs. In CQA QT24%, the modified R2 of 0.9312 is good compared to the predicted R2 of 0.7728. The precision ratio of 18.022 predicts a strong signal-to-noise ratio. Regarding PS, the precision ratio of 13.013 indicates a strong signal, but the expected R2 of 0.2945 is not close to the corrected R2 of 0.8687 since it may indicate a significant block effect. The overall mean, with an adjusted R2 of 0.7057, would be a better predictor of ZP than the predicted R2 of -1.0738. For PDI, even though the expected R2 of 0.0434 is not reached, a precision ratio of 8.697 suggests a sufficient signal.

Analysis for identification of overlay plot and design space

In the optimization case, the target decided in finding different QTPPs and CQAs was the preferred target assigned for different QT24%, PS, ZP, and PDI answers. Based on the essential quality goal product attributes, limits for different CQAs were established and processed for optimization (QTTP). In run 16, the Memantine-optimized PNs, 30 mg of Memantine, 30 mg of PLGA, 1.5% w/v poloxamer-188 concentration, and 10,000 rpm of stirring speed were used to achieve BBD. In the examination of the suggested optimized formulation, measurements included a QT24% of 77.946%, a PS of 148.899 nm, a ZP of 23.8 mV, and a PDI of 0.399. There were indications that the Memantine-optimized PNs could reach the QTTP with the optimal composition.

Characterization of Polymeric nanoparticles

Micromeritic studies

Table 3 lists the micrometric properties of lyophilized PNs: the % moisture content is 2.9 ± 0.5 and the angle of repose is 28.97 ± 1.6 degrees. Based on these micrometric data, run-16 was selected as the optimal formulation with the best flow characteristics.

Table 3: Carr's index, angle of repose, moisture content, and in-vivo pharmacokinetic parameters of pure drug and optimized formulation batch

Formulations	**Carr's index**	**Angle of repose (Θ)**	**Moisture Content (%)**	**C_{max} (µg/mL)**	**T max (h)**	**K_e**	**AUC∞0 (µg/h)/mL**	**t1/2**
Pure drug (MEM)	17.67 1.09	36.6 ±1.99	3.3 ± 0.32	0.672	3	191.774	11.458	0.0037
Optimized Formulation	13.21±0.99	28.97 ±1.6	2.9 ± 0.5	1.946	7	193.738	32.559	0.0036

Entrapment Efficiency

The results of all experiments Run-16 showed that Poloxamer-188 1.5% w/v at stirring speed of 10000 rpm had higher EE (70.57%) (i.e., Drug: PLGA concentration 30:30 mg).

Particle size and ZP determination

The zeta-sizer apparatus was used to measure the particle sizes of each formulation. The Memantine PNs had an optimized size range of 148.9 nm for Run-16 (Figure a). The Memantine-loaded PLGA-NP formulation that was produced had a uniform 200 nm particle size distribution and a spherical surface shape. Particle size may have been affected by the higher PLGA content, giving the impression that they are foggy (i.e., more aggregation). The ZP findings for the applicable formulation for Run-16 were 23.8 mV, as shown in the figure below.

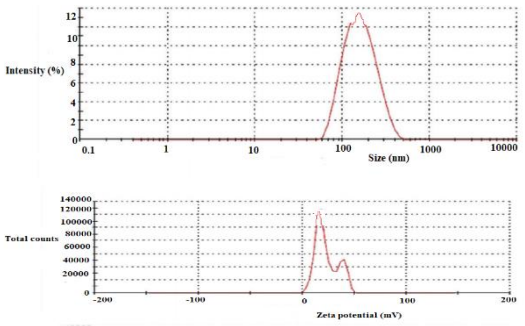

Fig. Particle size distribution and zeta potential curves of optimized formulation batch

Powder X-ray Diffraction (P-XRD)

The X-RD patterns of optimized PNs of Memantine and Memantine as a pure medicine are displayed in Figures a and b below. Memantine, a pure medication, confirmed a characteristic crystalline structure at a number of diffraction angles, including 6.56°, 12.7°, 14.5°, 17.2°, 19.1°, 22.3°, 25.1°, and 27.9°. Memantine's optimized photon counts (PNs) showed a decrease (minimum peak intensity at certain angles), indicating that the medication has an amorphous structure and is molecularly confined as a product that has been freeze-dried.

a) **b)**

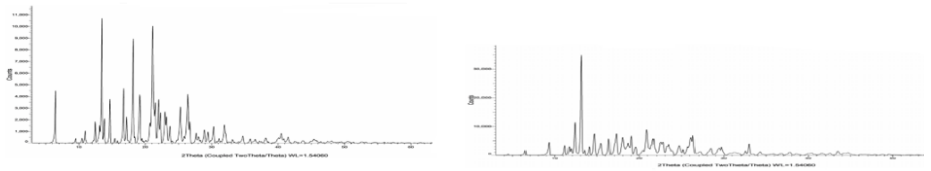

Fig. X-RD curves of pure drug (a) and optimized formulation batch (b) X-RD: X-ray diffraction

Scanning Electron Microscopy (SEM) and Transmission Electron Microscopy (TEM)

The scanning electron microscope images of Memantine in its purest form and its optimized PN form are displayed in Figures a and b below. In the SEM, Memantine appears as a rough surface with crystalline structures. However, as can be seen in the following image, the optimized particle numbers (PNs) of Memantine point to an amorphous form with spherical smooth-surfaced particles.

a) **b)**

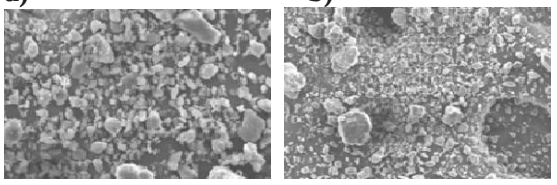

Fig. SEM images of optimized formulation batch (a) and pure drug (b) SEM: Scanning electron microscopy

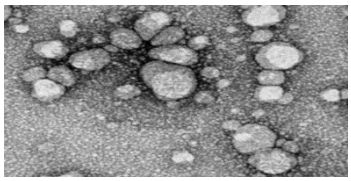

Fig. TEM image of optimized formulation batch TEM: Transmission electron microscopy

Thermogravimetric Analysis (TGA)

According to Memantine's TGA curve, the weight loss is found to be 0.046 mg with a percentage weight loss of 3.77 at a beginning temperature of 23°C. It then continues in a straight line with 1.43 mg and a percentage weight loss of 94.43 until the temperature reaches 280°C. Memantine's optimized PNs had a weight loss of 0.25 mg (or 9.23 percent weight loss) at 24°C according to the TGA curve. Subsequently, the curve had a steep decline at 180°C, resulting in a weight loss of 2.71 mg (58.59%), as illustrated in figures a and b below. The curve continued to decline until it reached 480°C, at which point it displayed a linear trend up to 800°C. Compared to the pure medication Memantine, this curve shows that the optimised formulation appears to be significant and thermo-stable in terms of weight loss.

a) **b)**

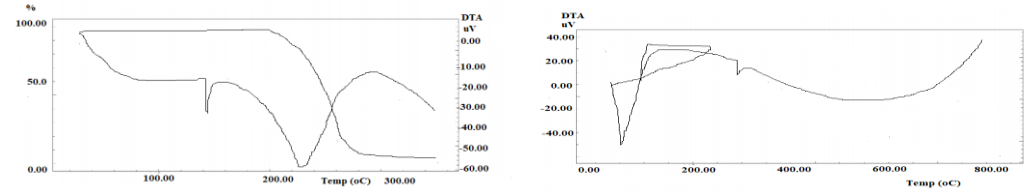

Fig. TGA plot of pure drug (a) and optimized formulation batch (b) TGA: Thermogravimetric analysis

Differential Thermal Analysis (DTA)

Memantine's DTA curve revealed a melting point at 302°C and a significant drop in peak intensity, indicating an endothermic reaction in connection to the melting point change. In other words, when optimized PNs showed a melting point of 312°C, it indicated that the optimized batch's peak of curvature had altered significantly as a result of the melting point shift at an enthalpy of 350.1 mJ. The optimized batch's endset enthalpy was determined to be at 68.32 °C and 21 °C, respectively, and these temperatures also had the largest onsets. The details of the DTA thermograms of the optimized PNs formulations and its pure drug, Memantine, are displayed in Figures a and b below.

a) **b)**

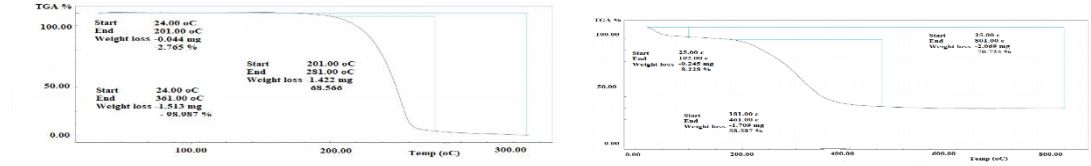

Fig. DTA plot of pure drug (a) and optimized formulation batch (b) DTA: Differential thermal analysis

In-vitro diffusion studies

The behaviour pattern of medication release for both pure medication and optimized medication PNs is shown in the following image. The drug release pattern found during in vitro diffusion studies for both pure drug and optimized drug-loaded PNs is depicted in the accompanying image. Following a six-hour testing, the graph showed that the optimized batch released the medicine around twice as much as the pure drug, indicating a considerable improvement in drug release. As a result, a medication that works well in combination with poloxamer-188 and PLGA has a better dissolving profile than the medication used alone. To fit kinetic models and comprehend the drug release process better, a variety of kinetic model equations are utilized, such as the zero-order, first-order, and Higuchi models. Following the application of such models, the R2 values for both drug-free and drug-loaded PNs were separately computed for each kinetic model. The optimised drug loaded PNs R2 values were determined to be 0.835, 0.868, and 0.944, respectively, compared to the obtained R2 values of 0.921 for pure drug, 0.934 for first-order, 0.940 for the Higuchi model, and 0.921 for zero-order. The Higuchi model for pure-drug Memantine and optimised PNs of Memantine appeared to be the best fit, according to the R2 values obtained for several kinetic models. For the pure drug Memantine and the optimised PNs of Memantine formulation, the release exponent (n) values were 0.689 and 0.478, respectively. As a result, whereas Memantine-optimized PNs exhibit non-Fickian diffusion kinetics, the drug release from pure drug exhibits Fickian diffusion kinetics.

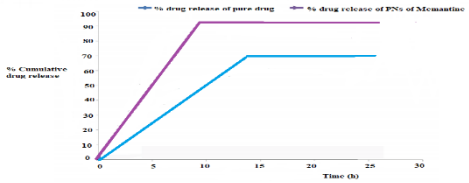

Fig. In-vitro drug release curve of pure drug vs. optimized formulation batch

Cytotoxicity studies

The cell viability of MEM-PLGA NPs was assessed using primary cultures of rat astrocytes and brain endothelial cells. Since these cells collectively comprise the blood-brain barrier, they are considered a suitable model to study the cytotoxicity of nanoparticles. After being incubated for 24 hours, MEM-PLGA NPs did not display any observable negative consequences, as the accompanying figure demonstrates. These results show that the generated particles and endothelial glial brain cells are biocompatible.

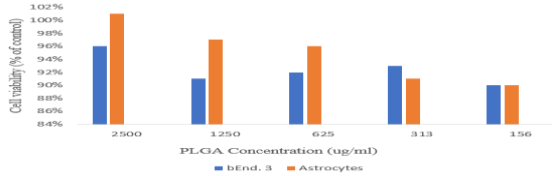

Fig. Cell viability assessment using Alamar blue on brain cell lines

In-vitro and in-vivo transport across the BBB

The in-vitro model's cell membrane preserved 40% of the initial MEM-PLGA NPs after 1 hour of incubation, while only 30% of the initial MEM was discovered inside the barrier, according to the results. In this model, Pe, the measure of drug permeability, was 0.934. This feature suggests that NPs kept in this tissue would be able to deliver the medicine either slowly from there or partially through it and into the basolateral media.

Morris water maze test

The MWM test was used to assess how the MEM therapy altered the animals' behaviour, as seen in the picture below. The overall ANOVA for the training days revealed that the mice's ability to learn spatially was affected by both the genotype (APP/PS1 against WT showed significant differences, p~<0.01) and the medication effect (treated vs. untreated APP/PS1 mice). The results of the escape latency test day are shown in Figure A. The group of untreated APP mice showed a substantially longer scape delay ($p < 0.01$) in comparison to the group receiving MEM-loaded NPs. In addition, mice treated with NPs showed improved spatial learning memory when compared to control mice (no statistically significant changes). This implies that using medication to treat AD is a feasible use for the developed Nanosystems. Compared to the other transgenic groups, the MEM-loaded NPs groups took a more direct route to the platform, as seen in Fig. b. As anticipated, there were significant differences between the MEM-loaded NPs and the APP/PS1 untreated group ($p < 0.01$). The time percentage in the platform quadrant indicates that MEM-loaded NPs restored cognition more successfully than the free medication: APP/PS1 animals treated with MEM-loaded NPs showed an average of 38.23% of the time there, whereas transgenic mice treated with MEM spent a 25.73% of the time there.

a) **b)**

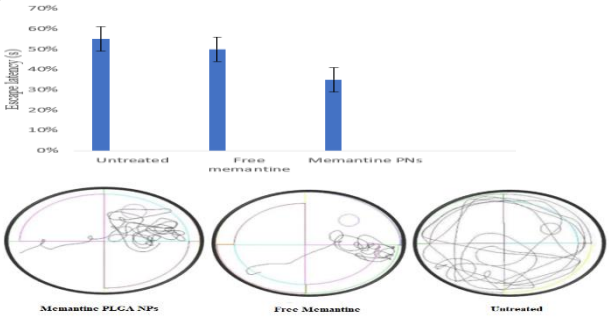

Fig. Morris water maze results on the probe trail of the APP/PS1 mice. a) Escape latency and b) representative swimming path of transgenic mice.

Immunohistochemistry

Researchers could see the emergence of A plaques, a pathologic feature of AD, thanks to the use of tiofavin-S staining. Several studies have demonstrated that MEM lowers the quantity of amyloid plaques; as a result, it would be crucial to carry out histology studies to track the formation of plaques. The accompanying figure (a) displays the results of amyloid plaque counting in APP/PS1 mice. In the WT groups, no amyloid plaques developed. Even so, the number of plaques produced in APP/PS1 mice treated with NPs was much lower than in the other transgenic groups ($p<0.001$ vs. untreated animals and $p<0.01$ vs. MEM mice). Figure B

displays the microscopic pictures of an insoluble plaque after Immunohistochemically staining. The amount of plaque development was higher in mice not administered APP. Furthermore, as is common with AD, there was a noticeable degree of inflammation surrounding the plaques. MEM-PLGA NPs groups showed reduced levels of inflammation and fewer plaques than other transgenic groups. These results suggest that MEM enhanced cognition by lowering AD-related inflammation and insoluble amyloid plaques. These results align with the results of behavioural tests.

a) **b)**

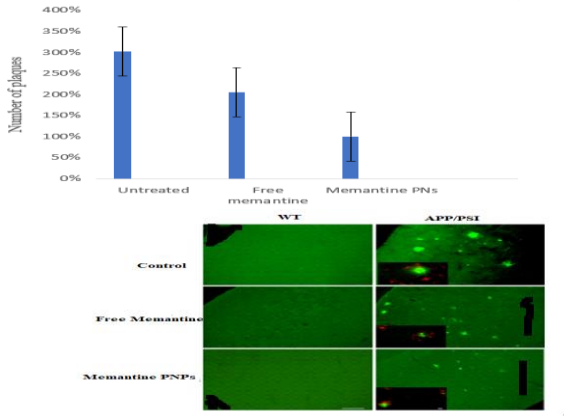

Fig. a) Immunohistochemically (cortex) staining of amyloid plaques (green) and GFAP (red) of WT and APP/PS1 mice (untreated, MEM free and MEM loaded NPs). Bar reference equivalent to 100 µm. and b Amyloid plaques counting of APP/PS1 mice

Accelerated stability outcomes

P values for the design from the accelerated stability studies are shown. The p value for each CQA was more than 0.05, meaning that there had not been a significant change. Since there were few to no appreciable changes in CQAs across the stability period, it was concluded that the optimised freeze-dried PNs of Memantine satisfied the stability criteria.

Method development

Different ratios of 20–50% acetonitrile and 0.1% formic acid were tested as the mobile phase for the LC-MS method. These trials showed non-resolved peaks in high organic ratios (both Memantine and NLB were eluted at 1.5 min) and separated forked peaks in low organic conditions (forked peaks for Memantine at 2.1 min and NLB at 3 min). Acetonitrile was tried in water without any acidification; the findings revealed two abnormally shaped peaks: a fronted Memantine peak at two minutes and a forked NLB peak at two minutes and thirty seconds. Using an ammonium formate buffer with a pH of 9.5 greatly enhanced peak shape, even though most current Memantine research uses acidic or neutral mobile phases; an alkaline pH predicts increased stability for Memantine and lessens its ionization to produce good separations on reverse phase columns. To match the sample matrix, methanol was utilized rather than acetonitrile. Two distinct methanol ratios—70% and 80%—were tested. The 70% methanol ratio produced good peak shapes with retention times of 2.5 and 8.5 minutes for Memantine and NLB, respectively; however, the 80% methanol ratio was the best ratio in terms of separation and run time, with retention times of 1.8 and 2.9 minutes for Memantine

and NLB, respectively. The column oven was set to 40 °C in order to speed up the separation process without sacrificing the stability of Memantine and NLB.

Peak areas in the atmospheric pressure chemical ionization mode (APCI), which showed a lower abundance of molecular ion peaks for both NLB and Memantine, were 43 times higher for NLB and 87 times higher for Memantine than in the electrospray ionization mode (ESI). NLB was chosen as IS due to its availability and structural similarity to Memantine. The following figure shows the architectures and fragmentation patterns of NLB and Memantine. To minimize band broadening and solvent mismatch, somewhat greater injection volumes were avoided; an ideal injection volume was 10 µL, or 1-4 percent of the column's empty capacity. To make the suggested approach simpler, direct protein precipitation was chosen as the sample treatment method rather than extraction techniques, in accordance with our lab's customs. Liquid-liquid extraction with diethyl ether was attempted, using 2 mL of ether to extract 100 µL of biological sample; however, no appreciable improvement was observed in chromatogram shapes or analytes recoveries (100 ng mL-1 solution showed 4% lower recovery from ether extraction compared to protein precipitation method).

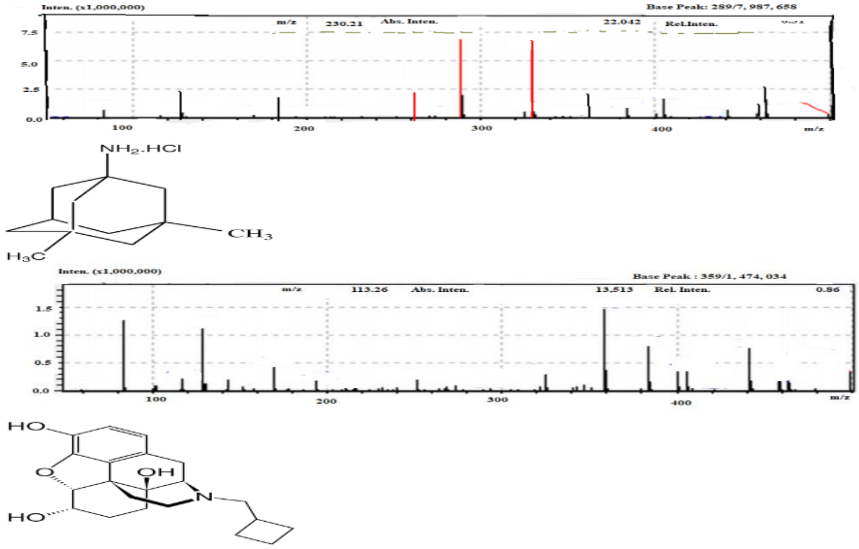

Fig. Memantine and b nalbuphine's structure and fragmentation pattern utilizing electrospray ionization (ESI) in positive mode from stock injection.

Base peaks—which are also protonated molecular ion peaks—are selected for additional single-ion monitoring (SIM) detection

Samples from the group treated with Memantine NP were first acidified in order to release the Memantine and dissolve the PLGA polymer. There were no discernible variations in the response factor between the acidification step-prepared standards and the regular standards. Two chromatograms for the same sample, with and without the acidification step, are displayed in the figure below. As shown, there is a substantial difference at the Memantine retention duration, indicating that the acidification step had an impact on the ability of the

samples from the Memantine-NP-treated groups to release the designated medication from PLGA nanoparticles.

a) **b)**

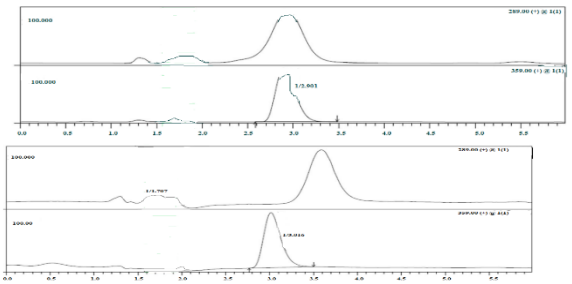

Fig. Chromatograms for brain homogenate samples taken from rats administered Memantine-NP dosage form a without sample preparation using acidification treatment and b with sample preparation using acidification treatment; the latter exhibiting a peak at Memantine retention.

Method validation

Selectivity and matrix effects

None of the blanks or zero calibrators showed any observable interference at the Memantine retention time. In blanks, a peak was seen at m/z 289 that was clearly distinct from Memantine and whose identification could not be determined with certainty using a single MS detection. However, it is postulated that they are biological matrices' interfering compounds, which are known to emerge during the analysis of tiny molecules from bio-fluids. There is no effect on trueness or precision due to the well-resolved interference peak. Additionally, blanks showed no interference at NLB retention time. The IS reaction in zero calibrators did not exceed by more than 5% the average NLB response of other calibrators and QCs. The next figures (a and b) show the blank and zero calibrator chromatograms in the brain homogenate matrix. All zero and blank calibrators from various matrices are shown in ESM.

a) **b)**

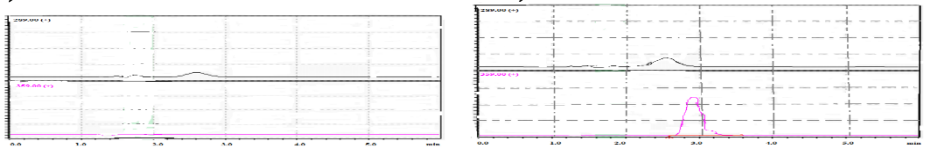

Linearity

Each matrix's Memantine concentration response relationships were fitted using a straightforward linear regression. Standard curves and line fit charts are part of ESM. In all three biological matrices, with correlation coefficient values (adjusted R2) in plasma, CSF, and brain homogenates, respectively, all residuals were distributed, percent deviations were less than 15% for all levels, and all regression parameters were approved (Table 4).

Table 4: Linearity parameters for Memantine response factor in different biological matrices

Parameter	Plasma	CSF	Brain

Range (ng mL-1)	0.5 – 300.0	0.5 – 300.0	0.5 – 300.0
Intercept (a)	−335.728	788.456	−743.288
Sa	3750.757	3724.873	5104.245
Slope (b)	3092.681	4674.896	3968.757
Sb	32.455	32.238	43.808
RSD% of the slope	1.018	0.669	1.080
Adjusted R square	0.9993	0.9997	0.9992
S y/x	9198.804	9136.307	12,520.147
F	9661.444	22,389.621	8592.246
Significance F	1.283 ×10-13	4.453 ×10-15	2.050 ×10-13

Sensitivity

When the analytical method is verified at LLOQ (0.5 ng mL-1) with less than 15% error in trueness and standard deviation, the required limit of 20% is satisfied. When the limit of detection (LOD) was investigated from noise, a discernible response of Memantine was discovered at 0.2 ng mL-1 analytical solution (shown in the subsequent figure).

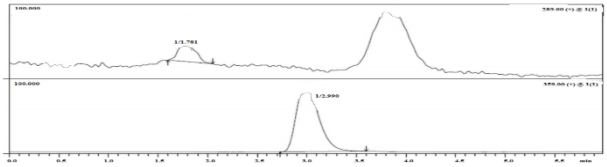

Fig. Limit of detection (LOD) was established using an LC chromatogram of a 0.2 ng mL-1 injection that demonstrated a noticeable peak response at Memantine retention with a signal to noise ratio greater than 3.

Stability

For the short term (bench top at room temperature for 6 h), freeze-thaw (3 cycles at −20 °C within a week), and post-preparative stability (processed samples in temperature-controlled auto sampler adjusted to 8 °C for 24 h), three sample sets at LLOQ (0.5 ng mL-1) and HQC (200 ng mL-1) were used. Each result deviated from the nominal concentrations by no more than 15%. However, a significant decrease in post-preparative stability in the 2 to 9 °C temperature range suggests that samples need to be injected immediately or stored at −20 °C. The response factor of two standard solutions (100 ng mL-1) made from two distinct stock solutions that were kept at -20 °C for ten months was used to compare the stability of the stock solution. The variation was 4.716%, or less than 5%, indicating that the supplies were stable at -20 °C.

Conclusion

After all, given their proven capacity to provide a more effective regimen, MEM-PLGA NPs seem to be a more practical alternative for treating AD patients than free MEM. P values for each CQA are used to differentiate between them, and an accelerated stability analysis of improved PNs confirms the minimal variations in the CQAs over a six-month storage period.

30 mg of Memantine, 30 mg of PLGA, and 1.5% w/v poloxamer-188 are the optimal dosages for the drug's PLGA-based PNs to have the intended effects, the study finds. I think this is a strong case.

References

1. Guttman R., Altman R.D., Nielsen N.H. Alzheimer disease: Report of the council on scientific affairs. Arch. Fam. Med. 1999; 8: 347–353.
2. Chopra K., Misra S., Kuhad A. Current perspectives on pharmacotherapy of Alzheimer's disease. Expert Opin. Pharm. 2011; 12: 335–350.
3. Oz M., Lorke D.E. Yang K., Petroianu G. On the interaction of β-amyloid peptides and α7-nicotinic acetylcholine receptors in Alzheimer's disease. Curr. Alzheimer Res. 2013; 10: 618–630.
4. Anand R., Gill K.D., Mahdi A.A. Therapeutics of Alzheimer's disease: Past, present and future. Neuropharmacology. 2014; 76: 27–50.
5. Ghavami A., Hirst W.D., Novak T.J. Selective phosphodiesterase (PDE)-4 inhibitors a novel approach to treating memory deficit? Drugs R D. 2006; 7: 63–71.
6. Meinert C., McCaffrey L.D., Breitner J.C.S. Alzheimer Disease Anti-Inflammatory Prevention Trial: Design, methods, and baseline results. Alzheimer's Dement. 2009; 5: 93–104.
7. Martinez A., Alonso M., Castro A., Perez C. First non-ATP competitive glycogen synthase kinase 3β (GSK-3β) inhibitors: Thiadiazolidinones (TDZD) as potential drugs for the treatment of Alzheimer's disease. J. Med. Chem. 2002; 45: 1292–1299.
8. Wischik C.M., Edwards P.C., Lai R.Y.K., Roth M., Harrington C.R. Selective inhibition of Alzheimer disease-like tau aggregation by phenothiazines. Proc. Natl. Acad. Sci. USA. 1996; 93: 11213–11218.
9. Analytical Method Development and Validation, a report by Jay Breaux, Kevin Jones and Pierre Boulas, AAI Development Services, United States.
10. U. S. Department of Health and Human Services, Food and Drug Administration. Guidance for Industry, Bioanalytical Method Validation, May 2001.
11. Xu RN, Fan L, Rieser M, El-Shourbagy TA. Recent advances in high-throughput quantitative bioanalysis by LC–MS/MS. Journal. Pharm. Biomed. Anal. 2007: 44(2): 342–355.
12. Pranay Wal. Method Development –Determination of Drugs in Biological Fluids. J. Pharm Sci and Tech. 2010: 2 (10), 333-347.
13. Kurz A., Grimmer T. Efficacy of Memantine hydrochloride once-daily in Alzheimer's disease. Exp Opin Pharmacother. 2014; 15(13):1955–60.
14. Matsunaga S., Kishi T., Iwata N. Memantine monotherapy for Alzheimer's disease: a systematic review and meta-analysis. PLoS ONE. 2015; 10(4):1–16.
15. Joshi G., Kumar A., Sawant K. Enhanced bioavailability and intestinal uptake of Gemcitabine HCl loaded PLGA nanoparticles after oral delivery. Eur J Pharm Sci. 2014; 60:80–9.
16. Zhu S., Chen S., Gao Y., Guo F., Li F., Xie B. Enhanced oral bioavailability of insulin using PLGA nanoparticles co-modified with cell-penetrating peptides and Engrailed secretion peptide. Drug Deliv. 2016; 23(6):1980–91.
17. Inchaurraga L., Martín-Arbella N., Zabaleta V., Quincoces G., Penuelas I., Irache JM. In vivo study of the mucus-permeating properties of PEG-coated nanoparticles following oral administration. Eur J Pharm Bio pharm. 2015; 97:280–9.
18. Xiaoqing XU., Guoguang C., Yaning LI., Jingjing W., Jun Y., Lili R. Enhanced dissolution and oral bioavailability of cinacalcet hydrochloride nanocrystals with no food effect. Nanotechnol. 2019; 30:55-102.
19. Swain S., Parhi R., Jena BR., Babu SM. Quality by design: concept to applications. Curr Drug Discov Technol. 2019; 16:240-250.

20. Padhi D., Harris R. Clinical pharmacokinetic and pharmacodynamics profile of cinacalcet hydrochloride. Clin Pharmacokinet. 2009; 48:303- 311.
21. Lammers T., Kiessling F., Hennink WE., Storm G. Drug targeting to Tumors: principles, pitfalls and (pre) clinical progress. J Control Release. 2012; 161:175-187.
22. Panigrahi KC., Patra CN. Rao MEB. Quality by design enabled development of oral self- nano emulsifying drug delivery system of a novel calcimimetic cinacalcet HCl using a porous carrier: in vitro and in vivo characterization. AAPS Pharm Sci Tech. 2019; 20:216.
23. Neupane YR., Sabir MD., Ahma N., and Ali M., Kohli K. Lipid drug conjugate nanoparticle as a novel lipid nanocarrier for the oral delivery of decitabine: ex vivo gut permeation studies. Nanotechnology. 2013; 24:415102.
24. Hu C., Rhodes DG. Proniosomes: a novel drug carrier preparation. Int J Pharm.1999; 185:23-35
25. Gregor C Mc., Bines E. The use of high-speed differential scanning calorimetry (Hyper- DSC) in the study of pharmaceutical polymorphs. Int J Pharm. 2007; 350:48-52.
26. Didem AS., Muharrem S, Johanna GW., Frank S., Thomas S. Nano structured Biomaterials and applications. J of Nanomater. 2016; 13.
27. Dynamic Light Scattering Particle Size and Zeta Potential Analyzer. Last Accessed Date: 03.11.2015.
28. Siepmann J., Siepmann F. Mathematical modelling of drug delivery. Int J Pharm. 2008; 364:328-343.
29. Lin SB., Hwang KS., Tsay SY., Cooper SL. Segmental orientation studies of polyether polyurethane block copolymers with different hard segment lengths and distributions. Colloid Polym Sci. 1985; 263:128-140.
30. Carter M., Jennifer S. In Guide to Research Techniques in Neuroscience. (2nd Ed). Marcel Dekker Inc; USA; 2015.
31. Peter Christoper GV., Vijaya Raghavan C., Siddharth K., Siva Selva KM., Hari Prasad R. Formulation and optimization of coated PLGA- zidovudine nanoparticles using factorial design and in-vitro in-vivo evaluations to determine brain targeting efficiency. Saudi Pharm. J 2014; 22:133-140
32. Haines PJ. Principles of thermal analysis and calorimetry, RSC paperbacks, Royal Soc of Chem. 2002:1-9.
33. Nakashima D., Takama H., Ogasawara Y., Kawakami T., Nishitoba T., Hoshi S., Uchida E., Tanaka H. Effect of cinacalcet hydrochloride, a new calcimimetic agent, on the pharmacokinetics of dextromethorphan: in vitro and clinical studies. J Clin Pharmacol. 2007; 47:1311-1319.
34. Differential thermal Analysis. Last Accessed Date: 01.12.2018.
35. Andreani T., Kiill CP., de Souza ALR., Fangueiro JF., Fernandes L., Doktorovová S, et al. Surface engineering of silica nanoparticles for oral insulin delivery: characterization and cell toxicity studies. Colloids Surf B Biointerfaces. 2014; 123:916–23.
36. Fangueiro JF., Andreani T., Egea MA., Garcia ML., Souto SB., Silva AM., et al. Design of cationic lipid nanoparticles for ocular delivery: development, characterization and cytotoxicity. Int J Pharm. 2014; 461(1–2):64–73.
37. Pedros I., Petrov D., Allgaier M., Sureda F., Barroso E., Beas-Zarate C., et al. Early alterations in energy metabolism in the hippocampus of APPswe/ PS1dE9 mouse model of Alzheimer's disease. Biochim Biophys Acta Mol Basis Dis. 2014; 1842(9):1556–66.